**Supplementary Material**

# Computational Discovery of Diverse Functionalities in Two-Dimensional Square Disulfide Monolayers: Auxetic Behavior, High Curie Temperature Ferromagnets, Electrocatalysts, and Photocatalysts

Yu Liu[1], Wenlong Li[1], Fengyu Li[1,*], Zhongfang Chen[2,*]

[1] *School of Physical Science and Technology, Inner Mongolia University, Hohhot, 010021, China*
[2] *Department of Chemistry, The Institute for Functional Nanomaterials, University of Puerto Rico, Rio Piedras Campus, San Juan, PR 00931, USA*

* Corresponding Authors: fengyuli@imu.edu.cn (FL); zhongfang.chen1@upr.edu (ZC)

**Table S1.** The structural parameters and cohesive energies of 68 *S*-$XS_2$ monolayers (the italics are the data of the corresponding hexagonal structure, and the bolds in $E_{coh}$ are the values of square structure larger than the corresponding hexagonal structure), where '*' indicates the cases where the optimized structures are not square.

| ***S*-XS₂** | ***a* = *b* (Å)** | ***h* (Å)** | ***θ* (°)** | $r_{X-S}$ (Å) | $E_{coh}$ (eV/atom) |
|---|---|---|---|---|---|
| *S*-$HS_2$ | 2.50 | 2.98 | 79.82 | 1.94 | 2.29 |
| | -- | -- | -- | -- | -- |
| *S*-$LiS_2$ | 2.60 | 4.00 | 65.91 | 2.38 | **2.90** |
| | *2.57/2.86* | *3.92* | *102.16* | *2.52* | *2.74* |
| *S*-$NaS_2$ | 2.70 | 4.66 | 60.03 | 2.69 | **2.39** |
| | *2.88* | *4.50* | *107.17* | *2.80* | *2.24* |
| *S*-$KS_2$ | 2.81 | 5.28 | 56.01 | 2.99 | 2.04 |
| | *2.51/4.77* | *3.69* | *72.65* | *3.12* | *2.23* |
| *S*-$RbS_2$ | 2.94 | 5.54 | 55.97 | 3.13 | **1.83** |
| | -- | -- | -- | -- | -- |
| *S*-$CsS_2$ | 5.00 | 4.19 | 100.12 | 3.26 | 1.22 |
| | *5.37* | *2.02* | *36.05* | *3.26* | *2.60* |
| *S*-$BeS_2$ | 2.81 | 3.07 | 84.94 | 2.08 | **3.58** |
| | *2.97* | *2.94* | *81.10* | *2.25* | *3.22* |
| *S*-$MgS_2$ | 3.05 | 3.78 | 77.67 | 2.43 | **2.84** |
| | *3.14* | *3.64* | *90.19* | *2.57* | *2.80* |
| *S*-$CaS_2$ | 3.32 | 4.21 | 76.54 | 2.68 | 2.96 |
| | *3.44* | *3.97* | *89.96* | *2.81* | *3.10* |
| *S*-$SrS_2$ | 3.59 | 4.39 | 78.52 | 2.84 | 2.69 |
| | *4.76* | *2.15* | *42.79* | *2.95* | *3.91* |
| *S*-$BaS_2$ | 4.13 | 4.19 | 89.19 | 2.94 | 2.65 |
| | *4.99* | *2.15* | *40.90* | *3.07* | *3.94* |
| *S*-$BS_2$ | 2.96 | 2.42 | 101.52 | 1.91 | **4.59** |
| | *4.17/2.96* | *3.20* | *64.41* | *1.91/3.52* | *4.59* |
| *S*-$AlS_2$ | 3.40 | 2.97 | 97.71 | 2.26 | **3.94** |
| | *3.45* | *2.76* | *69.41* | *2.43* | *3.74* |
| *S*-$GaS_2$ | 3.43 | 3.00 | 97.50 | 2.28 | **3.35** |
| | *3.46* | *2.91* | *72.03* | *2.47* | *3.04* |
| *S*-$InS_2$ | 3.66 | 3.31 | 95.70 | 2.47 | **3.01** |
| | *3.81* | *2.94* | *67.48* | *2.64* | *2.93* |
| *S*-$TlS_2$ | 3.76 | 3.40 | 95.72 | 2.54 | **2.50** |
| | *3.91* | *3.04* | *67.94* | *2.72* | *2.36* |
| *S*-$CS_2$ | 2.97 | 2.30 | 104.53 | 1.88 | 4.03 |
| | -- | -- | -- | -- | -- |
| ***S*-$SiS_2$** | 3.38 | 2.70 | 102.67 | 2.16 | **4.27** |
| | *3.24* | *2.91* | *75.80* | *2.37* | *3.77* |
| ***S*-$GeS_2$** | 3.51 | 2.85 | 101.90 | 2.26 | **3.68** |
| | *3.38* | *3.07* | *76.38* | *2.48* | *3.24* |
| ***S*-$SnS_2$** | 3.78 | 3.08 | 101.77 | 2.44 | **3.51** |
| | *3.61* | *3.26* | *76.12* | *2.64* | *2.71* |
| ***S*-$PbS_2$** | 3.94 | 3.20 | 101.77 | 2.54 | **3.05** |
| | *3.76* | *3.36* | *75.47* | *2.75* | *2.87* |

| | | | | | |
|---|---|---|---|---|---|
| *S*-$NS_2$ | 2.73 | 2.82 | 88.06 | 1.96 | 2.62 |
| | -- | -- | -- | -- | -- |
| **S*-$PS_2$ | 3.57/3.63 | 2.39 | 111.28 | 2.16 | **3.23** |
| | *3.16* | *3.12* | *81.06* | *2.40* | *2.94* |
| *S*-$AsS_2$ | 3.82 | 2.60 | 111.57 | 2.31 | **2.97** |
| | *3.33* | *3.33* | *81.66* | *2.54* | *2.80* |
| *S*-$SbS_2$ | 4.11 | 2.80 | 111.60 | 2.49 | **2.97** |
| | *3.61* | *3.41* | *78.63* | *2.69* | *2.91* |
| *S*-$BiS_2$ | 4.20 | 3.04 | 108.26 | 2.59 | **2.83** |
| | *3.77* | *3.50* | *77.53* | *2.79* | *2.81* |
| **S*-$OS_2$ | -- | -- | -- | -- | -- |
| *S*-$SeS_2$ | 3.87 | 2.78 | 108.58 | 2.38 | 2.46 |
| | *3.45* | *3.28* | *78.98* | *2.58* | *2.48* |
| *S*-$TeS_2$ | 4.37 | 2.45 | 121.50 | 2.50 | 2.63 |
| | *3.71* | *3.39* | *76.79* | *2.73* | *2.65* |
| *S*-$PoS_2$ | 4.12 | 3.29 | 102.85 | 2.64 | 2.68 |
| | *3.83* | *3.43* | *75.60* | *2.80* | *2.78* |
| **S*-$FS_2$ | -- | -- | -- | -- | -- |
| *S*-$ClS_2$ | 4.50 | 1.03 | 154.17 | 2.31 | 1.49 |
| | -- | -- | -- | -- | -- |
| *S*-$BrS_2$ | 4.53 | 1.70 | 138.77 | 2.42 | 1.51 |
| | -- | -- | -- | -- | -- |
| *S*-$IS_2$ | 4.68 | 1.98 | 134.05 | 2.54 | **1.74** |
| | *3.70* | *3.60* | *80.13* | *2.80* | *1.52* |
| **S*-$HeS_2$ | 2.31/2.46 | 7.64 | 35.67 | 4.01 | 0.61 |
| **S*-$NeS_2$ | 2.49/2.33 | 7.77 | 32.81 | 4.13 | 1.78 |
| **S*-$ArS_2$ | 2.69/2.55 | 8.32 | 34.06 | 4.35 | 1.27 |
| **S*-$KrS_2$ | 2.69/2.86 | 8.14 | 38.78 | 4.30 | 0.90 |
| **S*-$XeS_2$ | -- | -- | -- | -- | -- |
| *S*-$ScS_2$ | 3.68 | 3.22 | 97.62 | 2.44 | 4.44 |
| | *3.79* | *2.72* | *63.68* | *2.58* | *4.69* |
| ***S*-$TiS_2$** | 3.68 | 2.71 | 107.15 | 2.29 | 5.00 |
| | *3.35* | *3.02* | *75.97* | *2.45* | *5.10* |
| ***S*-$VS_2$** | 3.53 | 2.64 | 107.72 | 2.21 | 4.53 |
| | *3.17* | *2.97* | *78.07* | *2.36* | *4.82* |
| ***S*-$CrS_2$** | 3.50 | 2.48 | 109.38 | 2.15 | 3.78 |
| | *3.04* | *2.94* | *79.82* | *2.29* | *4.17* |
| ***S*-$MnS_2$** | 3.44 | 2.44 | 109.44 | 2.11 | 3.65 |
| | *3.11* | *2.77* | *75.37* | *2.27* | *3.84* |
| *S*-$FeS_2$ | 3.46 | 2.33 | 112.15 | 2.08 | 3.89 |
| | *3.15* | *2.66* | *72.35* | *2.25* | *3.99* |
| *S*-$CoS_2$ | 3.52 | 2.23 | 115.29 | 2.08 | 3.86 |
| | *3.23* | *2.51* | *67.73* | *2.25* | *3.98* |
| *S*-$NiS_2$ | 3.67 | 2.05 | 121.57 | 2.10 | 3.71 |
| | *3.55* | *2.11* | *54.42* | *2.30* | *3.93* |
| *S*-$CuS_2$ | 2.66 | 3.82 | 69.79 | 2.33 | 3.08 |
| | *3.72* | *2.14* | *52.95* | *2.40* | *3.13* |
| **S*-$ZnS_2$ | 2.55/3.72 | 3.44 | 105.19 | 2.34 | 2.55 |

| | | | | | |
|---|---|---|---|---|---|
| *S*-$YS_2$ | 3.94 | 3.44 | 98.55 | 2.60 | 4.44 |
| | *4.07* | *2.82* | *61.93* | *2.74* | *4.82* |
| ***S*-$ZrS_2$** | 3.93 | 2.87 | 107.67 | 2.43 | 5.45 |
| | *3.58* | *3.15* | *74.59* | *2.60* | *5.57* |
| *S*-$NbS_2$ | 3.72 | 2.81 | 105.87 | 2.33 | 5.39 |
| | *3.35* | *3.12* | *77.88* | *2.48* | *5.80* |
| ***S*-$MoS_2$** | 3.71 | 2.61 | 109.73 | 2.27 | 4.51 |
| | *3.18* | *3.13* | *80.78* | *2.41* | *5.41* |
| *S*-$TcS_2$ | 3.58 | 2.65 | 106.98 | 2.23 | 4.65 |
| | *3.29* | *2.90* | *74.66* | *2.39* | *4.90* |
| *S*-$RuS_2$ | 3.63 | 2.51 | 110.63 | 2.21 | 4.57 |
| | *3.34* | *2.80* | *71.98* | *2.38* | *4.65* |
| *S*-$RhS_2$ | 3.67 | 2.46 | 112.27 | 2.21 | 4.08 |
| | *3.34* | *2.86* | *72.82* | *2.32* | *4.16* |
| *S*-$PdS_2$ | 2.70 | 4.16 | 65.91 | 2.48 | 3.03 |
| | *3.92* | *2.07* | *49.07* | *2.48* | *3.32* |
| *S*-$AgS_2$ | 2.71 | 4.53 | 61.73 | 2.64 | **2.53** |
| | *3.41* | *3.22* | *78.70* | *2.54* | *2.31* |
| *S*-$CdS_2$ | 3.09 | 4.06 | 74.60 | 2.55 | 2.09 |
| | *5.12/4.29* | *2.16* | *39.74* | *3.37/2.47* | *2.49* |
| *S*-$HfS_2$ | 3.82 | 2.91 | 105.41 | 2.40 | 5.52 |
| | *3.54* | *3.13* | *74.93* | *2.57* | *5.66* |
| *S*-$TaS_2$ | 3.69 | 2.83 | 105.05 | 2.33 | 5.46 |
| | *3.34* | *3.13* | *78.04* | *2.48* | *5.91* |
| *S*-$WS_2$ | 3.53 | 2.88 | 101.51 | 2.28 | 5.20 |
| | *3.19* | *3.14* | *80.93* | *2.42* | *5.91* |
| ***S*-$ReS_2$** | 3.63 | 2.61 | 108.63 | 2.24 | 4.76 |
| | *3.32* | *2.88* | *73.77* | *2.40* | *4.85* |
| ***S*-$OsS_2$** | 3.67 | 2.47 | 112.03 | 2.21 | 4.84 |
| | *3.38* | *2.77* | *70.88* | *3.39* | *5.01* |
| *S*-$IrS_2$ | 3.77 | 2.34 | 116.41 | 2.22 | **4.53** |
| | *3.36* | *2.88* | *72.83* | *2.32* | *4.43* |
| *S*-$PtS_2$ | 3.54 | 2.84 | 102.52 | 2.27 | 3.72 |
| | *3.48* | *2.79* | *69.64* | *2.45* | *3.75* |
| *S*-$AuS_2$ | 3.38 | 3.34 | 90.73 | 2.37 | 2.46 |
| | *4.70/3.41* | *3.23* | *46.72* | *4.08/4.07* | *2.86* |
| **S*-$HgS_2$ | 4.05/2.71 | 3.91 | 61.11 | 2.67 | 1.68 |

**Table S2.** The elastic constants (in $Nm^{-1}$), Young's modulus ($Y$, in $Nm^{-1}$) and Poisson's ratio ($v$) of the 37 thermodynamically and dynamically stable *S*-$XS_2$ structures, including 27 mechanically stable monolayers and 10 mechanically unstable monolayers. Negative Poisson's ratios are indicated in bold within the data, while relevant data for two $SiS_2$ structures obtained by the CALYPSO code are represented in italics.

| | $C_{11}$ | $C_{22}$ | $C_{12}$ | $C_{66}$ | $Y_x$ | $Y_y$ | $v_x$ | $v_y$ |
|---|---|---|---|---|---|---|---|---|
| *S*-$BS_2$ | 102.62 | 102.62 | 27.83 | 20.47 | 95.08 | 95.08 | 0.271 | 0.271 |
| *S*-$AlS_2$ | 47.97 | 47.97 | 2.91 | 4.77 | 47.79 | 47.79 | 0.061 | 0.061 |
| *S*-$GaS_2$ | 45.58 | 45.58 | 4.24 | 6.69 | 45.19 | 45.19 | 0.093 | 0.093 |
| *S*-$InS_2$ | 33.21 | 33.21 | 3.47 | 2.70 | 32.85 | 32.85 | 0.104 | 0.104 |
| *S*-$TlS_2$ | 24.02 | 24.02 | 2.93 | 3.34 | 23.85 | 23.85 | 0.121 | 0.121 |
| *S*-$SiS_2$ | 96.37 | 96.37 | −5.18 | 2.13 | 96.09 | 96.09 | **−0.054** | **−0.054** |
| *$SiS_2$-2* | *97.11* | *91.33* | *−2.76* | *7.04* | *81.41* | *76.57* | ***−0.030*** | ***−0.028*** |
| *$SiS_2$-3* | *115.12* | *115.12* | *24.97* | *45.07* | *109.70* | *109.70* | *0.217* | *0.217* |
| *S*-$GeS_2$ | 75.55 | 75.55 | −4.73 | 1.72 | 75.26 | 75.26 | **−0.063** | **−0.063** |
| *S*-$SnS_2$ | 51.39 | 51.39 | −4.27 | 0.98 | 51.04 | 51.04 | **−0.083** | **−0.083** |
| *S*-$PbS_2$ | 39.49 | 39.49 | −2.45 | 0.09 | 39.34 | 39.34 | **−0.062** | **−0.062** |
| *S*-$TiS_2$ | 31.38 | 31.38 | 0.51 | 5.05 | 31.37 | 31.37 | 0.016 | 0.016 |
| *S*-$VS_2$ | 28.55 | 28.55 | 3.38 | 7.49 | 28.15 | 28.15 | 0.118 | 0.118 |
| *S*-$CrS_2$ | 40.30 | 40.30 | 10.91 | 11.31 | 37.35 | 37.35 | 0.271 | 0.271 |
| *S*-$MnS_2$ | 42.33 | 42.33 | 10.85 | 10.85 | 39.55 | 39.55 | 0.256 | 0.256 |
| *S*-$FeS_2$ | 12.65 | 12.65 | −7.20 | 6.52 | 8.55 | 8.55 | **−0.569** | **−0.569** |
| *S*-$CoS_2$ | 20.67 | 20.67 | 11.32 | 3.69 | 14.47 | 14.47 | 0.548 | 0.548 |
| *S*-$ZrS_2$ | 29.70 | 29.70 | 0.44 | 1.78 | 29.69 | 29.69 | 0.015 | 0.015 |
| *S*-$NbS_2$ | 22.19 | 22.19 | 15.42 | 7.03 | 11.48 | 11.48 | 0.695 | 0.695 |
| *S*-$MoS_2$ | 44.10 | 44.10 | 12.71 | 8.54 | 40.44 | 40.44 | 0.288 | 0.288 |
| *S*-$RuS_2$ | 39.25 | 39.25 | 15.13 | 2.45 | 33.41 | 33.41 | 0.385 | 0.385 |
| *S*-$RhS_2$ | 13.98 | 13.98 | −6.20 | 3.90 | 11.23 | 11.23 | **−0.443** | **−0.443** |
| *S*-$AgS_2$ | 145.48 | 145.48 | −11.17 | 0.31 | 144.62 | 144.62 | **−0.077** | **−0.077** |
| *S*-$HfS_2$ | 37.67 | 37.67 | 3.75 | 1.57 | 37.30 | 37.30 | 0.100 | 0.100 |
| *S*-$TaS_2$ | 27.43 | 27.43 | 20.19 | 8.59 | 12.57 | 12.57 | 0.736 | 0.736 |
| *S*-$WS_2$ | 22.66 | 22.66 | 19.85 | 13.86 | 5.27 | 5.27 | 0.876 | 0.876 |
| *S*-$ReS_2$ | 29.96 | 29.96 | 11.82 | 9.71 | 25.30 | 25.30 | 0.395 | 0.395 |
| *S*-$OsS_2$ | 37.47 | 37.47 | 15.20 | 2.66 | 31.30 | 31.30 | 0.406 | 0.406 |
| *S*-$IrS_2$ | 34.27 | 34.27 | 6.90 | 3.57 | 32.88 | 32.88 | 0.201 | 0.201 |
| ***Mechanically unstable*** | | | | | | | | |
| *S*-$BeS_2$ | 52.22 | 52.22 | 53.49 | 8.99 | -- | -- | -- | -- |
| *S*-$AsS_2$ | −131.99 | −131.99 | 189.29 | 2.51 | -- | -- | -- | -- |
| *S*-$SbS_2$ | −43.02 | −43.02 | 82.43 | 1.36 | -- | -- | -- | -- |
| *S*-$BiS_2$ | 8.07 | 8.07 | 25.83 | 0.63 | -- | -- | -- | -- |
| *S*-$NiS_2$ | −19.25 | −19.25 | −45.40 | 6.65 | -- | -- | -- | -- |
| *S*-$CuS_2$ | −29.58 | −29.58 | −3.50 | 4.63 | -- | -- | -- | -- |
| *S*-$TcS_2$ | 15.42 | 15.42 | 15.83 | 9.42 | -- | -- | -- | -- |
| *S*-$CdS_2$ | −4.37 | −4.37 | 53.28 | 4.26 | -- | -- | -- | -- |
| *S*-$PtS_2$ | −34.02 | −34.02 | −25.91 | −3.46 | -- | -- | -- | -- |
| *S*-$AuS_2$ | 22.16 | 22.16 | 12.80 | −1.54 | -- | -- | -- | -- |

$C_{11} = C_{22}$.

Young's moduli $Y_x = Y_y = (C_{11}C_{22} - C_{12}C_{21})/C_{11}$

Poisson's ratio $v_x = v_y = C_{12}/C_{11}$

**Table S3.** Possible stable structures predicted by CALYPSO code arranged in descending order based on cohesive energy ($E_{coh}$).

| number | $E_{coh}$ (eV/atom) | space group | top-view | side-view |
|---|---|---|---|---|
| 1 | 4.27 | *P*-4*m*2 | 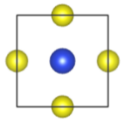 | 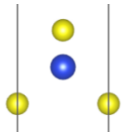 |
| 2 | 4.26 | *C*222 | 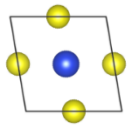 | 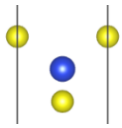 |
| 3 | 4.24 | *P*-3*m*1 | 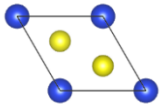 | 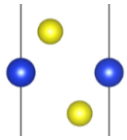 |
| 4 | 4.17 | *C*2 | 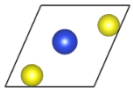 | 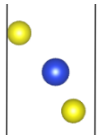 |

**Table S4.** Bader and Hirshfeld (in italic) charge analysis of *S*-$XS_2$ (X = Si, Ge, Sn, Pb, Ti, V, Cr, Mn, Zr, Mo, Re, Os) monolayers (in |*e*|).

| *S*-$XS_2$ | X | S | *S*-$XS_2$ | X | S |
|---|---|---|---|---|---|
| *S*-$SiS_2$ | +2.31/+*0.26* | −1.15/−*0.13* | *S*-$CrS_2$ | +1.10/+*0.28* | −0.55/−*0.14* |
| *S*-$GeS_2$ | +1.24/+*0.28* | −0.62/−*0.14* | *S*-$MnS_2$ | +0.94/+*0.02* | −0.47/−*0.01* |
| *S*-$SnS_2$ | +1.44/+*0.41* | −0.72/−*0.20* | *S*-$ZrS_2$ | +1.97/+*0.38* | −0.99/−*0.19* |
| *S*-$PbS_2$ | +1.04/+*0.46* | −0.52/−*0.23* | *S*-$MoS_2$ | +1.14/+*0.30* | −0.57/−*0.15* |
| *S*-$TiS_2$ | +1.69/+*0.28* | −0.84/−*0.14* | *S*-$ReS_2$ | +0.91/+*0.06* | −0.46/−*0.03* |
| *S*-$VS_2$ | +1.43/+*0.17* | −0.72/−*0.09* | *S*-$OsS_2$ | +0.61/+*0.04* | −0.31/−*0.02* |

**Table S5.** Relative energies of antiferromagnetic (AFM) and ferromagnetic (FM) states relative to non-magnetic (NM) state in a 2×2×1 supercell of *S*-$XS_2$ (X = Re, Os, Si, Ge, Sn, Pb, Zr, Ti, Mo, V, Cr, and Mn) monolayers. Bold highlighting indicates monolayers with the lowest energies. The primary cell lattice constants (*a*) of the magnetic ground state of the *S*-$XS_2$ (X = Mo, V, Cr, and Mn) monolayers.

| | $E_{AFM1} - E_{NM}$ (eV) | $E_{AFM2} - E_{NM}$ (eV) | $E_{FM} - E_{NM}$ (eV) | *a* (Å) |
|---|---|---|---|---|
| *S*-$ReS_2$ | 0.00 | 0.00 | 0.00 | -- |
| *S*-$OsS_2$ | 0.00 | 0.00 | 0.00 | -- |
| *S*-$SiS_2$ | 0.00 | 0.00 | 0.00 | -- |
| *S*-$GeS_2$ | 0.00 | 0.00 | 0.00 | -- |
| *S*-$SnS_2$ | 0.00 | 0.00 | 0.00 | -- |
| *S*-$PbS_2$ | 0.00 | 0.00 | 0.00 | -- |
| *S*-$ZrS_2$ | 0.00 | 0.00 | 0.00 | -- |
| *S*-$TiS_2$ | 0.00 | 0.00 | 0.00 | -- |
| *S*-$MoS_2$ | **−0.91** | 0.00 | −0.04 | 7.41 |
| *S*-$VS_2$ | −1.70 | −1.54 | **−1.96** | 3.65 |
| *S*-$CrS_2$ | −4.44 | −3.61 | **−5.43** | 3.66 |
| *S*-$MnS_2$ | −3.28 | −2.88 | **−3.79** | 3.75 |

**Table S6.** $\Delta G_{H^*}$ values (in eV) for H adsorption at different sites on the same side of *S*-$XS_2$ (X = Re, Os, Cr, and Mn) monolayers. Certain initial sites transform to more stable geometries after relaxation. Values closest to zero are highlighted in bold.

| *S*-$XS_2$ | S1 | S2 | S3 | S4 | S5 | S6 | S7 | S8 |
|---|---|---|---|---|---|---|---|---|
| *S*-$ReS_2$ | 0.72 | S1 | 0.78 | S5 | **0.17** | S7 | 0.95 | 0.95 |
| *S*-$OsS_2$ | 0.81 | S1 | 0.93 | S5 | **0.46** | S7 | 0.47 | 0.48 |
| *S*-$CrS_2$ | 0.15 | S1 | S1 | S8 | S8 | S8 | S8 | **−0.37** |
| *S*-$MnS_2$ | −0.11 | S1 | S1 | S8 | S8 | S7 | −0.12 | **−0.49** |

**Table S7.** $\Delta G_{H^*}$ values (in eV) for H adsorption at various sites on the antiferromagnetic (AFM1) *S*-$MoS_2$ monolayer. Certain initial sites transform to more stable geometries after relaxation. Values closest to zero are highlighted in bold.

| *S*-$XS_2$ | S1 | S2 | S3 | S4 | S5 | S6 |
|---|---|---|---|---|---|---|
| *S*-$MoS_2$ | S8 | S8 | 0.95 | S5 | 0.36 | S8 |
| S7 | S8 | S9 | S10 | S11 | S12 | S13 |
| S8 | **0.23** | S8 | 0.36 | S10 | 0.95 | S1 |

**Table S8.** $\Delta G_{H^*}$ values (in eV) of the *S*-$XS_2$ monolayers at various H coverage ($\theta$) conditions. The data in brackets represent the $\Delta G_{H^*}$ values of the corresponding magnetic ground state after H adsorption.

| H coverage ($\theta$) | *S*-$ReS_2$ | *S*-$OsS_2$ | *S*-$CrS_2$ | *S*-$MnS_2$ | *S*-$MoS_2$ |
|---|---|---|---|---|---|
| 1/4 | 0.17 | 0.46 | −0.37 | −0.49 | 0.23 (0.37) |
| 1/9 | −0.06 | 0.03 | −0.38 | −0.50 | -- |
| 1/16 | −0.18 | −0.09 | −0.41 | −0.52 | 0.09 (0.32) |

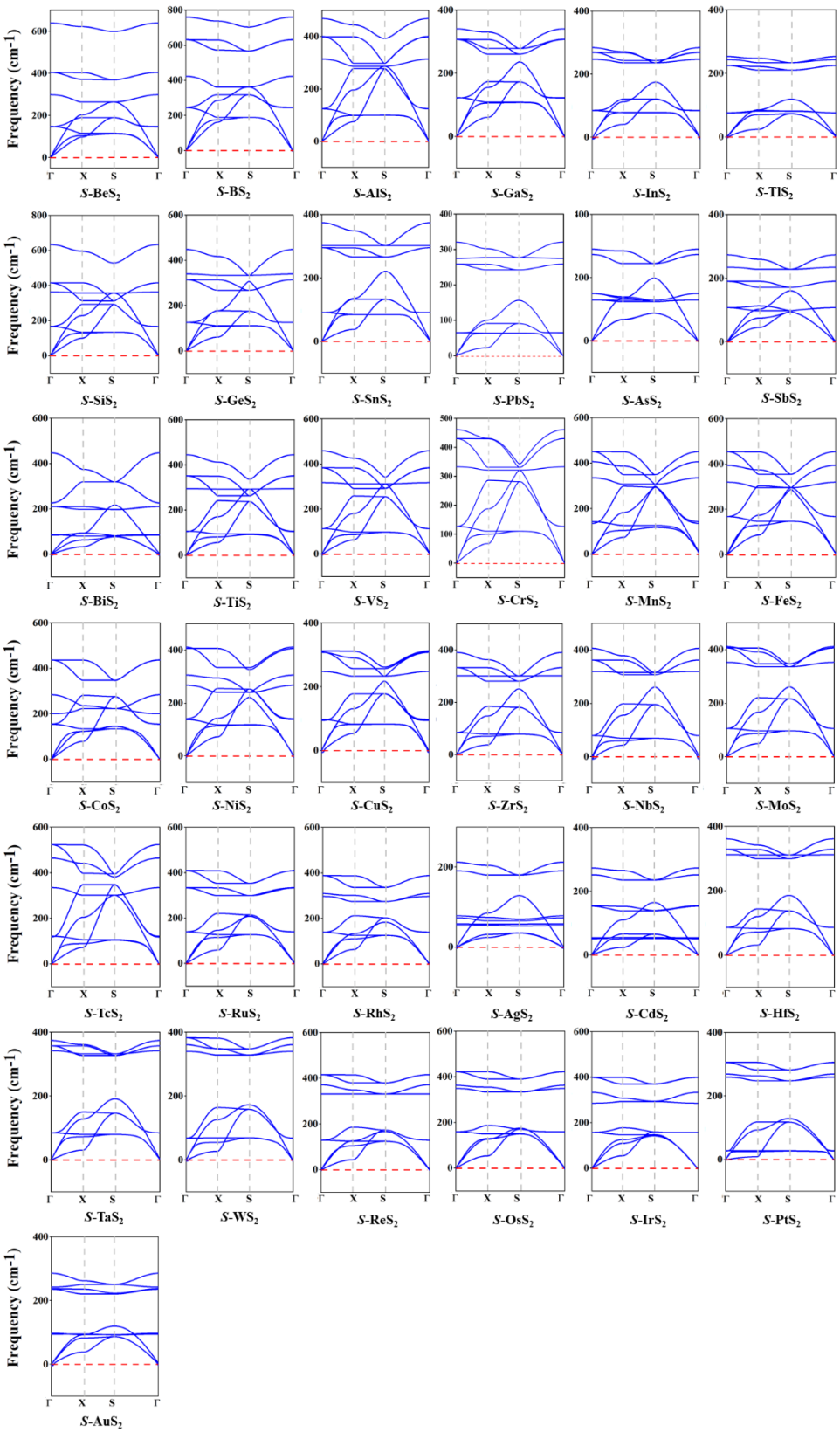


**Fig. S1** Calculated phonon dispersion curves of the 37 dynamically stable *S*-$XS_2$ monolayers.

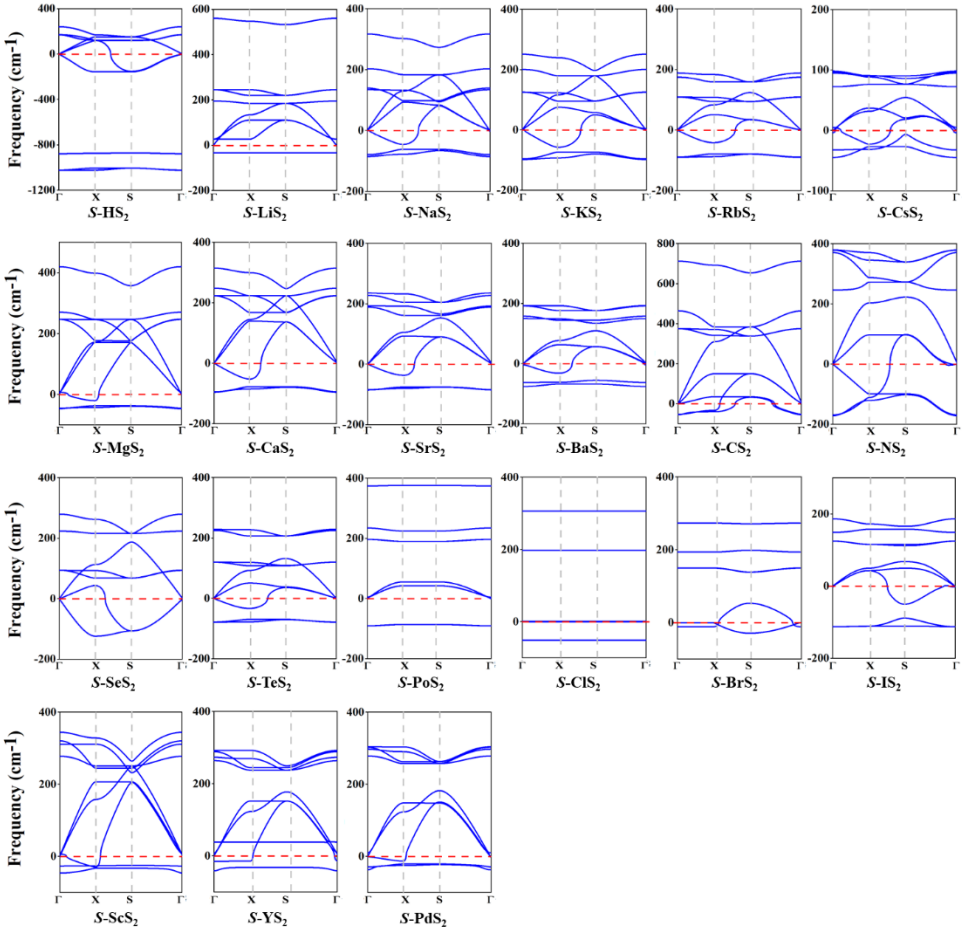


**Fig. S2** Calculated phonon dispersion curves of 21 *S*-$XS_2$ monolayers with significant imaginary frequencies.

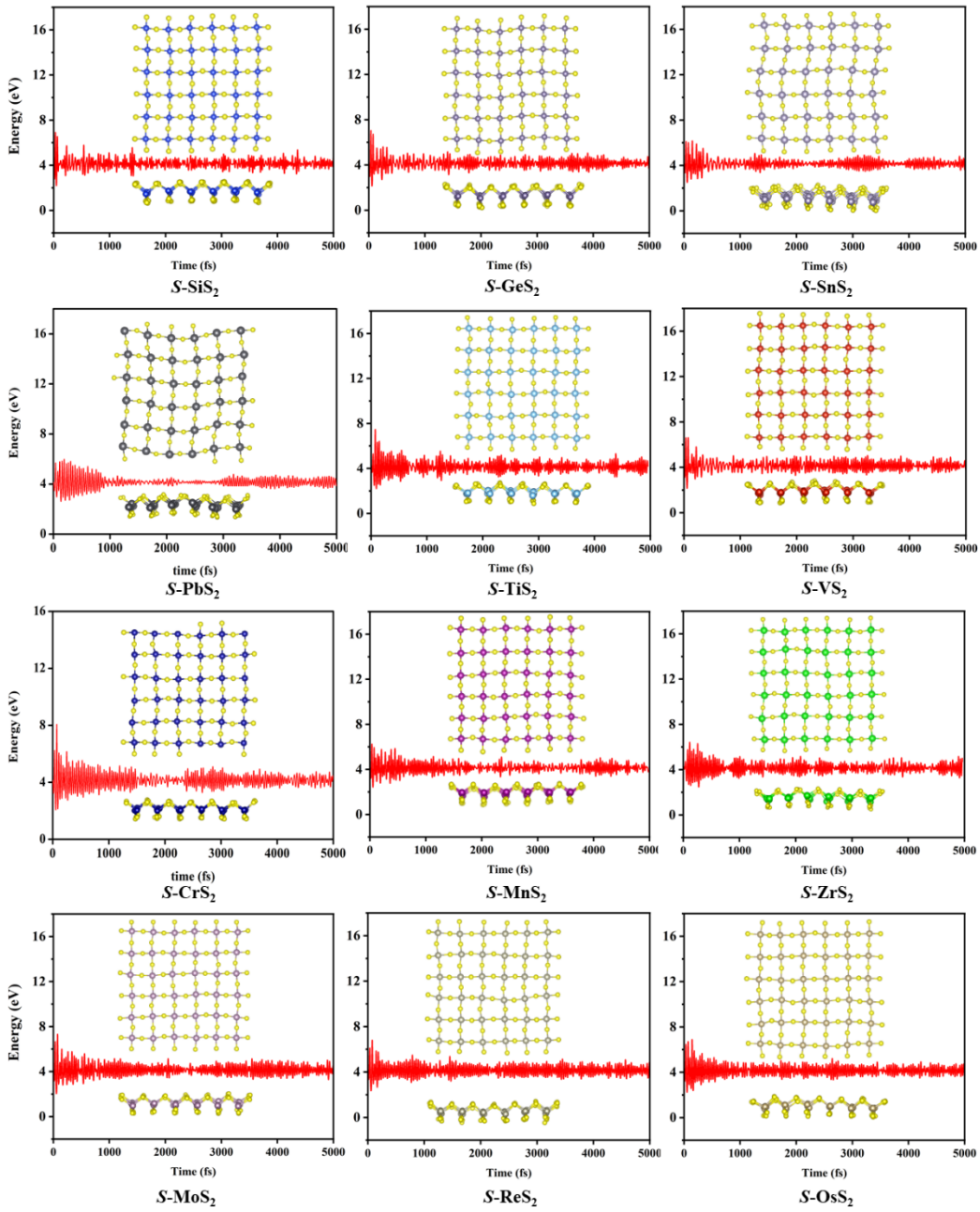


**Fig. S3** Final structure and energy fluctuation of 12 thermally stable *S*-$XS_2$ monolayers upon 5 ps FPMD simulations at 300 K.

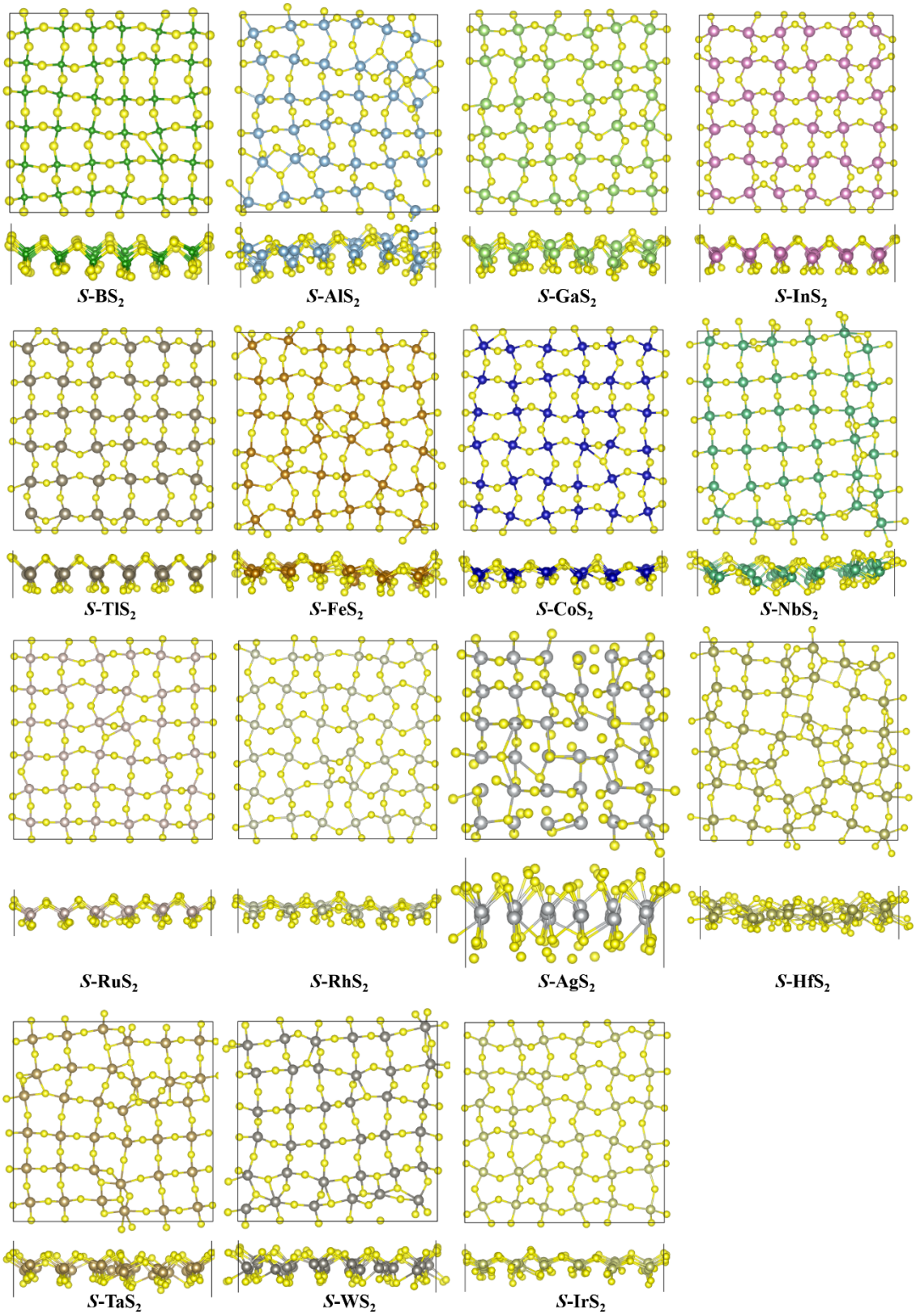


**Fig. S4** Final structures of 15 thermally unstable *S*-$XS_2$ monolayers after 5 ps FPMD simulations at 300 K.

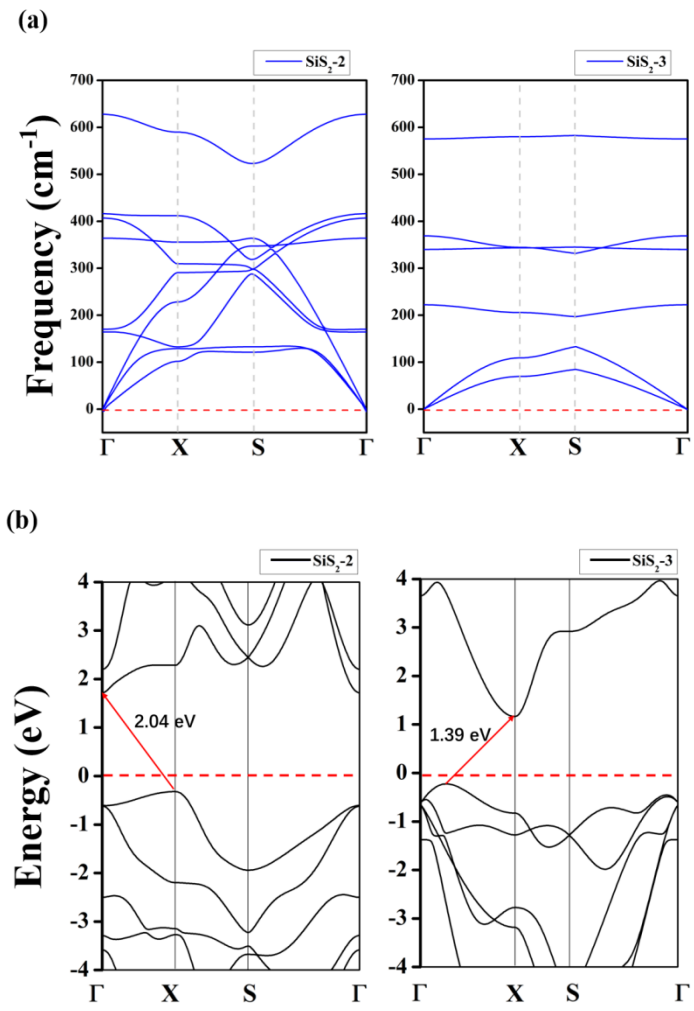


**Fig. S5** (a) Phonon spectra and (b) band structures of $SiS_2$-2 and $SiS_2$-3.

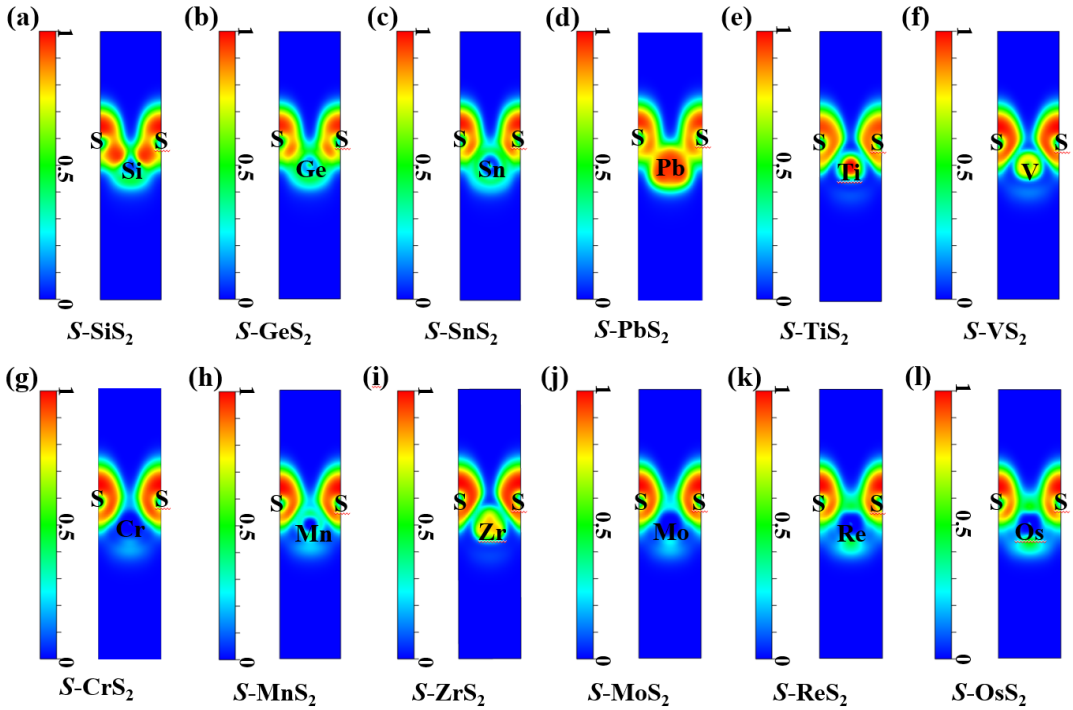


**Fig. S6** ELF maps of (010) slice for the square monolayer. ELF = 1 (red) and 0 (blue) indicate the accumulated and vanished electron densities, respectively. (a) *S*-$SiS_2$, (b) *S*-$GeS_2$, (c) *S*-$SnS_2$, (d) *S*-$PbS_2$, (e) *S*-$TiS_2$, (f) *S*-$VS_2$, (g) *S*-$CrS_2$, (h) *S*-$MnS_2$, (i) *S*-$ZrS_2$, (j) *S*-$MoS_2$, (k) *S*-$ReS_2$, and (l) *S*-$OsS_2$.

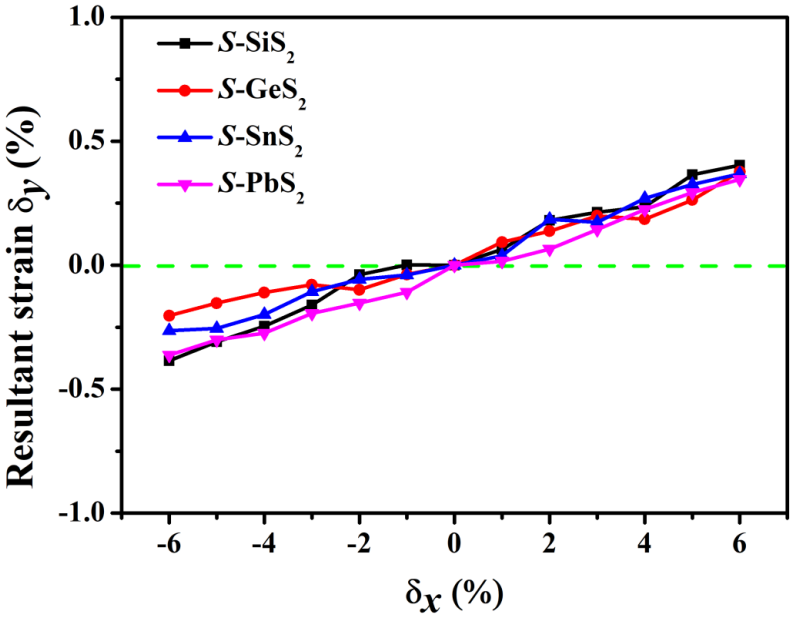


**Fig. S7** Mechanical response of the *S*-$XS_2$ (X = Si, Ge, Sn, and Pb) monolayers under the uniaxial (ranging from −6% to 6%) strain along the *x*-direction.

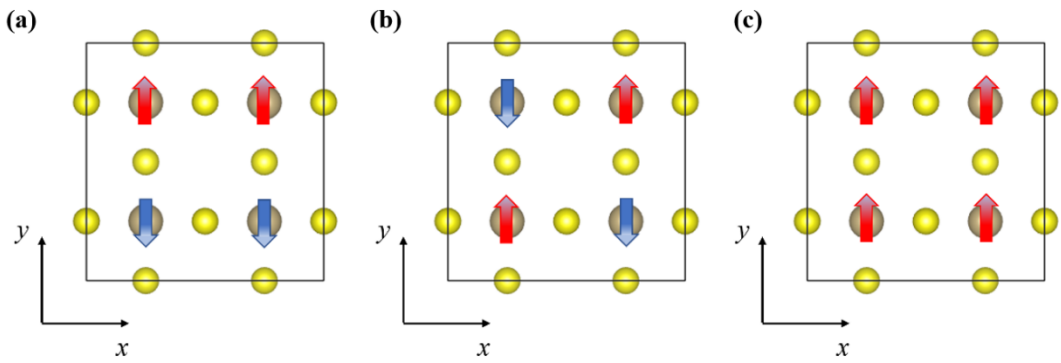


**Fig. S8** Schematic illustration of three different magnetic orders of *S*-$XS_2$ monolayer. (a) AFM1. (b) AFM2. (c) FM.

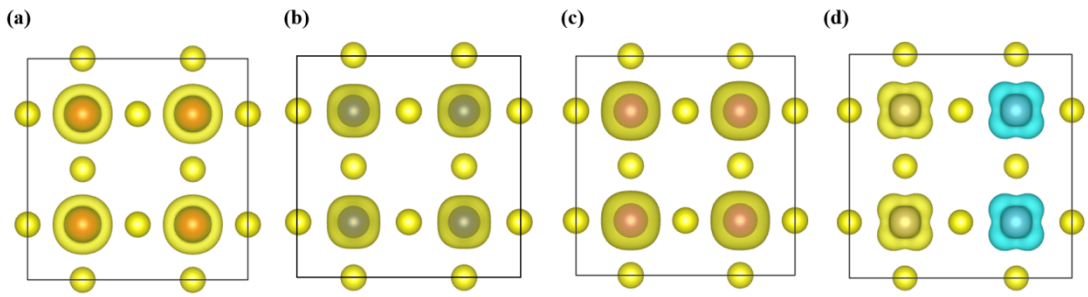


**Fig. S9** Magnetism distribution of metal atoms in *S*-$VS_2$, *S*-$MnS_2$ and *S*-$MoS_2$ monolayers. The isosurface values were set as 0.02 e $Å^{-3}$. (a) V atom in *S*-$VS_2$ (1.39 $\mu_B$) monolayer. (b) Cr atom in *S*-$VS_2$ (2.91 $\mu_B$) monolayer. (c) Mn atom in *S*-$MnS_2$ (3.28 $\mu_B$) monolayer. (d) Mo atom in *S*-$MoS_2$ (±1.46 $\mu_B$) monolayer.

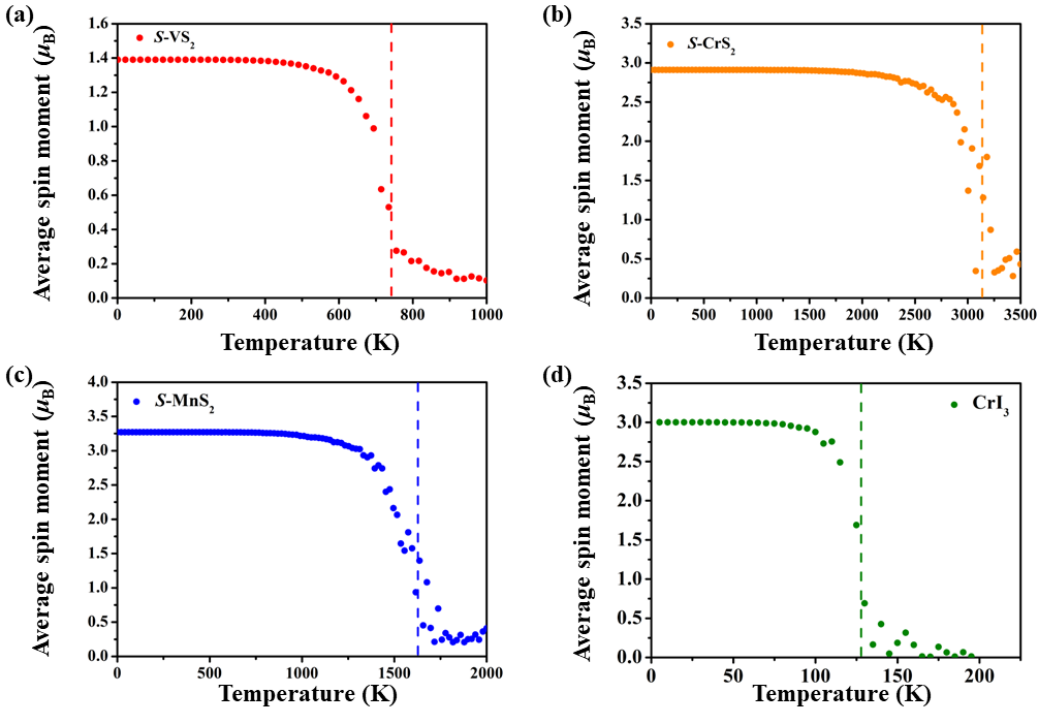


**Fig. S10** On-site magnetic moments of transition metal atoms as a function of temperature from MC simulations. (a) *S*-$VS_2$. (b) *S*-$CrS_2$. (c) *S*-$MnS_2$. (d) $CrI_3$.

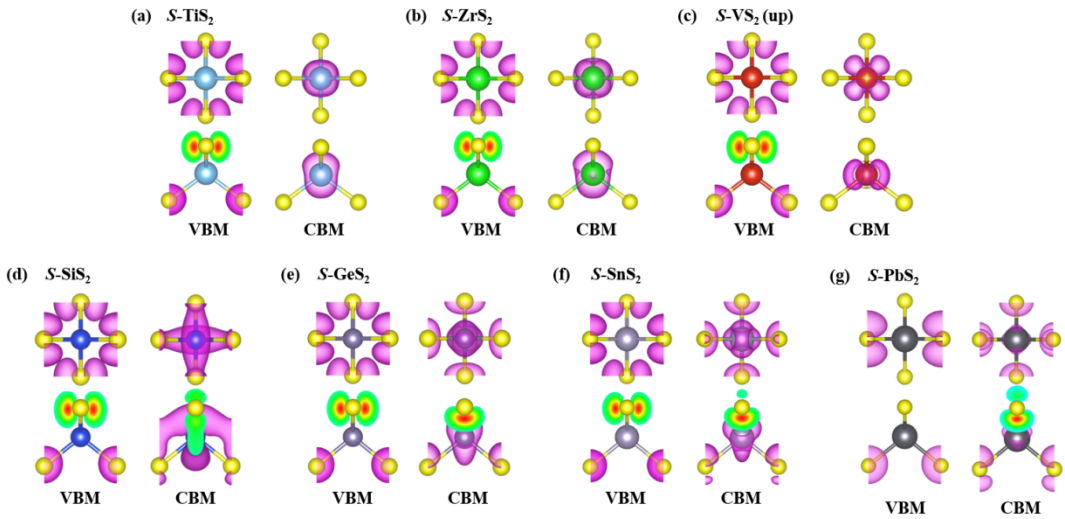


**Fig. S11** Partial charge distribution of VBM and CBM of *S*-$XS_2$ monolayers. (a) *S*-$TiS_2$. (b) *S*-$ZrS_2$. (c) *S*-$VS_2$ (spin-up channel). (d) *S*-$SiS_2$. (e) *S*-$GeS_2$. (f) *S*-$SnS_2$. (g) *S*-$PbS_2$. The isosurface values were set as 0.01 e $Å^{-3}$.

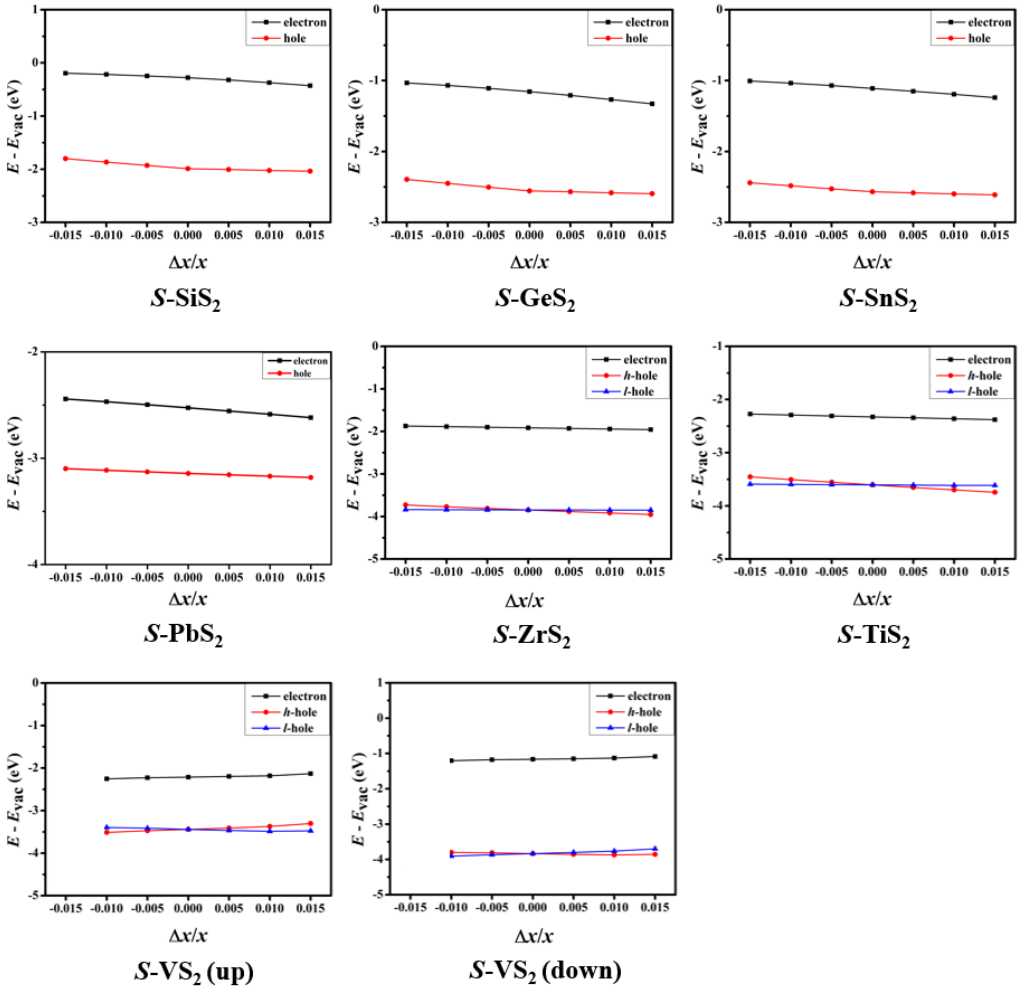


**Fig. S12** Fitting curves of deformation potentials of *S*-$XS_2$ (X = Si, Ge, Sn, Pb, Zr, Ti, and V (spin-up and spin-down)) monolayers. The strain ($\Delta x/x$) is ranging from −0.015 to 0.015 with the steps of 0.005.

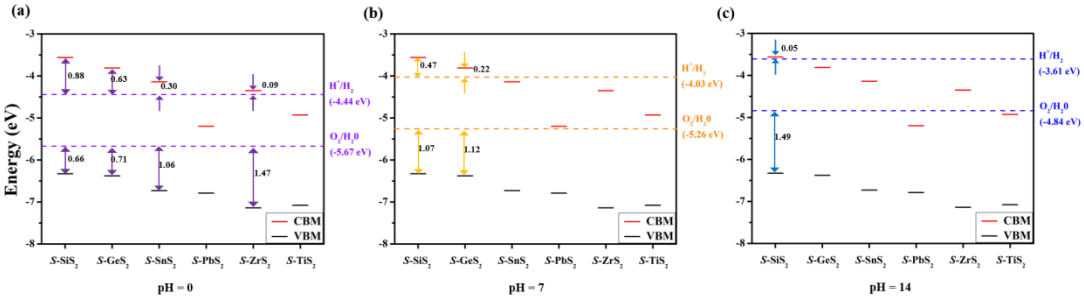


**Fig. S13** CBM and VBM energies of *S*-$XS_2$ (X = Si, Ge, Sn, Pb, Zr, and Ti) monolayers. Redox potentials of water splitting at (a) pH = 0 (purple dashed lines), (b) pH = 7 (orange dashed lines), and (c) pH = 14 (blue dashed lines).

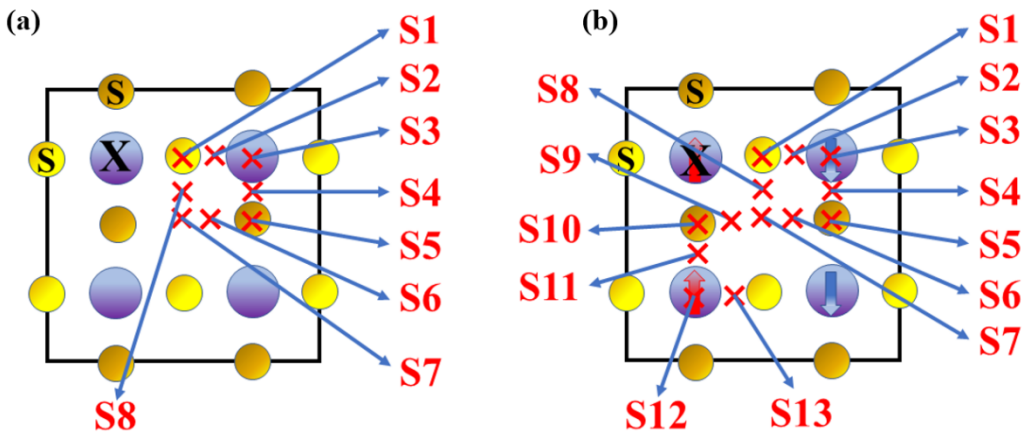


**Fig. S14** (a) Possible H adsorption sites on the nonmagnetic (NM) *S*-$ReS_2$, *S*-$OsS_2$ and ferromagnetic (FM) *S*-$MnS_2$ monolayers with a 2×2×1 supercell. (b) Possible H adsorption sites on the antiferromagnetic (AFM1) *S*-$MoS_2$ monolayer, the red/blue arrow indicate the spin up/down magnetic configuration of Mo. Purple and dark/light yellow balls represent the X and S atoms of bottom/top layer, respectively.

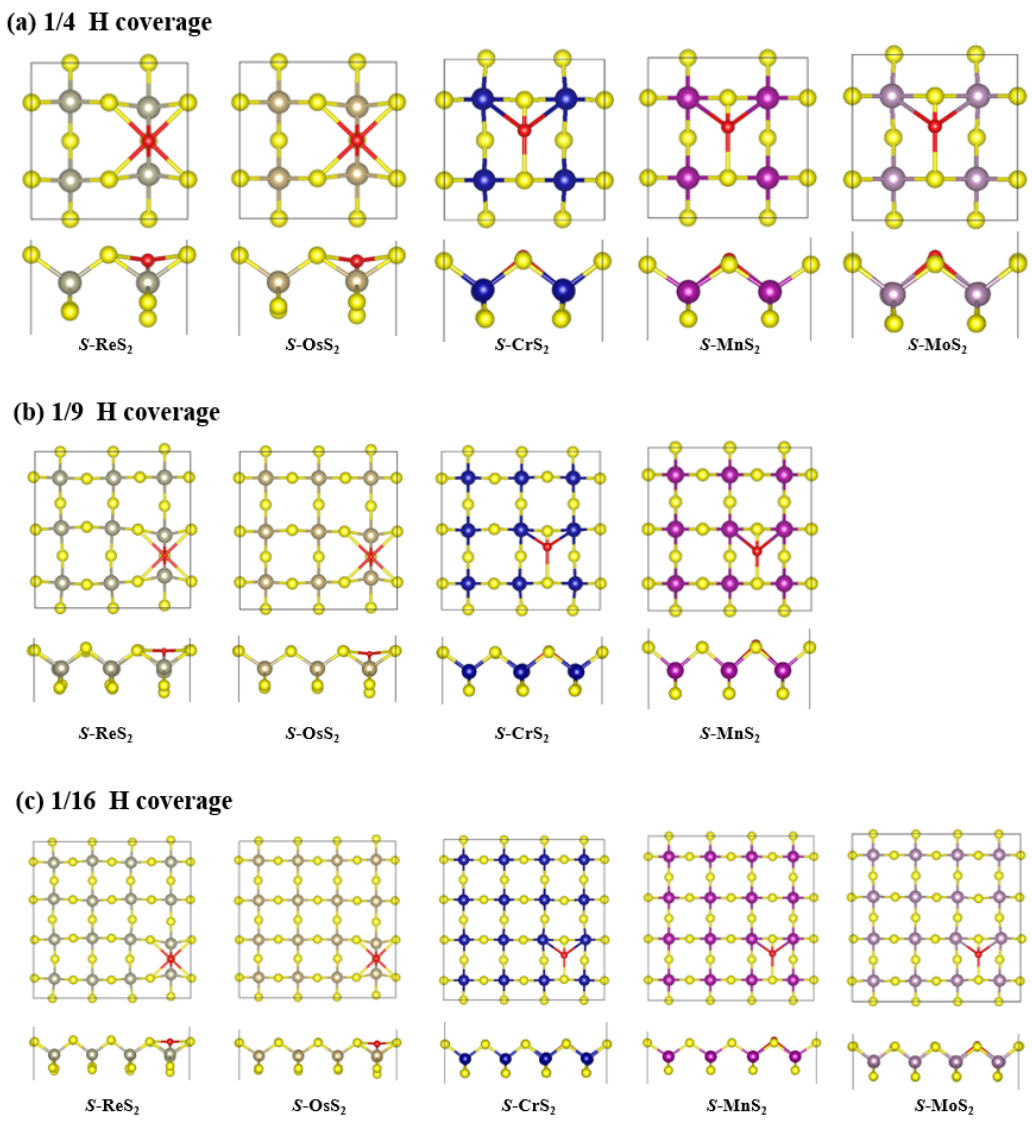


**Fig. S15** Optimized structures of the energetically most favorable H adsorption sites on the *S*-$XS_2$ (X = Re, Os, Cr, Mo, and Mn) monolayer with H coverage of (a) 1/4, (b) 1/9 and (c) 1/16.